Available online at www.sciencedirect.com
ScienceDirect
ELSEVIER
International Journal of Heat and Mass Transfer 50 (2007) 1982–1992
International Journal of HEAT and MASS TRANSFER
www.elsevier.com/locate/ijhmt

Analysis on the cooling performance of the thermoelectric micro-cooler

Kong Hoon Lee *, Ook Joong Kim

Energy Systems Research Center, Korea Institute of Machinery and Materials, Daejeon 305-343, Republic of Korea

Received 10 July 2006
Available online 15 December 2006

Abstract

Numerical analysis has been carried out to figure out the performance of the thermoelectric micro-cooler with the three-dimensional model. A small-size and column-type thermoelectric cooler is considered and Bi_2Te_3 and Sb_2Te_3 are selected as the n- and p-type thermoelectric materials, respectively. The thickness of a thermoelectric element considered is 5–20 μm. The effect of parameters such as the temperature difference, the current, the thickness of a thermoelectric element, and the number of thermoelectric pairs on the performance of the cooler has been investigated. The predicted results show that the performance can be improved for the thick element with the large number of thermoelectric pairs or the small cross-sectional area of the element.
© 2006 Elsevier Ltd. All rights reserved.

1. Introduction

Thermoelectric devices are used for both cooling and power generation using the Peltier and Seebeck effects, respectively [1]. The thermoelectric device contains over hundreds of n–p couples connected electrically in series, but thermally in parallel between two planar substrates. Because the Peltier and Seebeck effects are directly related, the best materials for the cooling are also optimized for power generation. Near room temperature, the most efficient materials are heavily doped p-type and n-type $(Bi,Sb)_2Te_3$.

Advance in the fabrication technique with micro-electromechanical systems (MEMS) technology has made it possible to fabricate a lot of micro-devices. Some of such devices require the precise thermal management and the compact cooling system for effective cooling within a small volume. The thermoelectric micro-cooler has become a promising candidate due to its cooling power density higher than that of the conventional bulk cooler [2,3]. Thermoelectric micro-cooler can easily be integrated and it is a suitable technique for the effective cooling of such devices as it does not have any moving parts.

The thermoelectric micro-cooler requires a structure difficult to produce with conventional techniques and the fabrication with MEMS techniques has been attempted. Yao et al. [4,5] developed the analytical model for the in-plain type thermoelectric micro-cooler and fabricated the cooler with both Si/Ge superlattice and Bi_2Te_3 for spot cooling. Snyder et al. [6] reported that they fabricated the thermoelectric micro-device using the electrochemical deposition with the photoresist mould. They used 400-μm-thick oxidized silicon as a substrate and formed 20-μm-thick thermoelectric elements (Bi_2Te_3 for p-type and Sb_2Te_3 for n-type). Böttner et al. [7] fabricated the micro-cooler using their new fabrication technique using the 4 in. wafer and reported that a net cooling of about 11 K was achieved using ~800 mA with 3 p/n-junctions. da Silva and Kaviany [8] carried out the one-dimensional theoretical analysis for the column-type thermoelectric micro-cooler to be used in the cooling of the vapor sensor. They also fabricated the micro-cooler based on the analysis and measured the performance of the cooler [9].

In order to figure out the performance of the thermoelectric cooler the three-dimensional numerical analysis has been carried out. The development of the model follows the one-dimensional approach of da Silva and

* Corresponding author. Fax: +82 42 868 7335.
E-mail addresses: konghoon@kimm.re.kr (K.H. Lee), ojkim@kimm.re.kr (O.J. Kim).

0017-9310/$ - see front matter © 2006 Elsevier Ltd. All rights reserved.
doi:10.1016/j.ijheatmasstransfer.2006.09.037

Nomenclature

A_{te}	cross-sectional area of a single thermoelectric element (m^2)
COP	coefficient of performance
J_e	electric current (A)
j_e	electric current density (A/m^2)
k	thermal conductivity (W/m K)
L	thickness (m)
N_{te}	number of thermoelectric elements
P	strength of electron/hole–phonon interaction (W/m^2 K)
P_e	electric power (W)
Q_c	cooling rate at the cold-side substrate (W)
Q_h	heat release rate at the hot-side substrate (W)
q	heat flux (W/m^2)
R_e	electrical resistance (Ω)
R_c	thermal conduction resistance (K/W)
T	temperature (°C or K)
V	voltage (V)
z	coordinate (m)

Greek symbols

α_{bulk}	bulk Seebeck coefficient (V/K)
α_b	boundary Seebeck coefficient (V/K)
ρ_e	electrical resistivity (Ω m)

Subscripts

b	boundary
c	cold, contact
cold	cold substrate
e	electron
h	hot, contact
i	index
hot	hot substrate
p	phonon
te	thermoelectric element

Kaviany [8] and extends it to three-dimensional situation. The COMSOL Multiphysics[1] is utilized in the analysis, which is a software package applicable to multiphysics problems. The small-size and column-type thermoelectric cooler is considered. It is known that tellurium compounds currently have the highest cooling performance around room temperature. Thus, in the present study, Bi_2Te_3 and Sb_2Te_3 are selected as the n- and p-type thermoelectric materials, respectively. The thermoelectric element considered has the thickness of 5–20 μm. The thickness of the element affects the thermal and electrical transport through the interface between the thermoelectric element and metal connector. The effect of parameters such as the temperature difference, the current, the thickness of the thermoelectric element, and the number of thermoelectric pairs on the performance of the micro-cooler has also been investigated. The coefficient of performance (COP) is the primary factor to evaluate the performance of the cooler and the COP varies with the parameters.

2. Analysis

The physical domain firstly considered in the present study is composed of two silicon substrates and 24 thermoelectric elements sandwiched between two substrates as shown in Fig. 1. The size of each substrate is 560 μm × 380 μm × 200 μm. The thermoelectric element is 20 μm thick and is located between the top and bottom metal connectors of 2 μm thick. The thickness of the thermoelectric element is changed to 5, 10, or 15 μm in the analysis to figure out the effect of the thickness on the cooling performance.

The analysis is carried out with the different governing equations for the substrates and thermoelectric elements, respectively. Heat transfer in the materials which do not have the thermoelectric features is accomplished by conduction of free electrons. However, in the thermoelectric materials, the electron–phonon thermal non-equilibrium is caused near the boundary due to the phonon and electron boundary resistances at the metal and thermoelectric interface [8]. The energy conversion mechanisms such as the Joule heating and Peltier cooling/heating will also contribute to this non-equilibrium [10].

2.1. Model for the thermoelectric element

The model development follows the one-dimensional approach of da Silva and Kaviany [8] and extends it to three-dimensional situation. The governing equations are obtained from the kinetics of electrons and phonons in an electric field or an temperature field which is described by the coupled Boltzmann equations for electrons and phonons [8,10,11]. The equations are generally written as

$$-\nabla\cdot(k_p\nabla T_p) = P(T_e - T_p), \tag{1}$$

$$-\nabla\cdot(k_e\nabla T_e) = \rho_e j_e^2 - P(T_e - T_p), \tag{2}$$

where j_e is the electric current density, P represents the strength of the electron/hole–phonon interaction, which is obtained with the density of electrons/holes, Boltzmann constant, and electron/hole energy relaxation time [8,10].

The electrical and thermal contact resistances at the interface between the thermoelectric element and metal

[1] See http://www.comsol.com

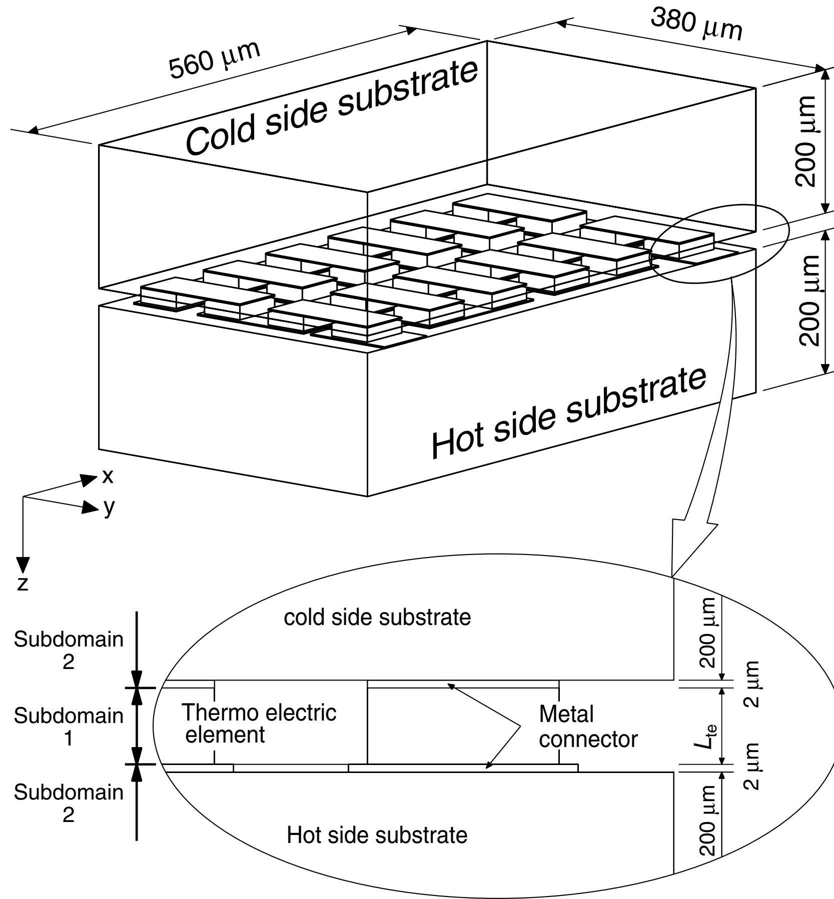

Fig. 1. Schematic of the thermoelectric cooler.

connector are considered in the model. The contact resistances cause the temperature jump through the interface and this phenomenon is treated with the interface conditions considering the resistances. The interface conditions for phonon conduction are as follows:

$$\left.\frac{T_c - T_p}{(A_{te}R_c)_{b,p}}\right|_{-\frac{L_{te}}{2}} = -k_p \left.\frac{\partial T_p}{\partial z}\right|_{-\frac{L_{te}}{2}}, \quad (3)$$

$$\left.\frac{T_p - T_h}{(A_{te}R_c)_{b,p}}\right|_{\frac{L_{te}}{2}} = -k_p \left.\frac{\partial T_p}{\partial z}\right|_{\frac{L_{te}}{2}}. \quad (4)$$

The interface conditions for electron conduction are as follows:

$$\left.\frac{T_c - T_e}{(A_{te}R_c)_{b,e}}\right|_{-\frac{L_{te}}{2}} = -k_e \left.\frac{\partial T_e}{\partial z}\right|_{-\frac{L_{te}}{2}} + \Delta\alpha j_e T_e|_{-\frac{L_{te}}{2}} - (A_{te}R_e)_b \frac{j_e^2}{2}, \quad (5)$$

$$\left.\frac{T_e - T_h}{(A_{te}R_c)_{b,e}}\right|_{\frac{L_{te}}{2}} = -k_e \left.\frac{\partial T_e}{\partial z}\right|_{\frac{L_{te}}{2}} + \Delta\alpha j_e T_e|_{\frac{L_{te}}{2}} + (A_{te}R_e)_b \frac{j_e^2}{2}, \quad (6)$$

where $\Delta\alpha = \alpha_{bulk} - \alpha_b$ and both α_{bulk} and α_b are given in Table 1. The terms in the left hand side of the above equations represent the heat flow as defined by the phonon (electron) boundary resistance. The second terms in the right hand side of Eqs. (5) and (6) represent the Peltier cooling and heating, respectively. The third terms represent the Joule heating at the interfaces. Adiabatic boundary conditions are applied to all the boundary surfaces except for the interfaces indicated in Eqs. (3)–(6).

Table 1
Properties of (Panel a) n- and p-type thermoelectric elements [8], (Panel b) metal connectors and silicon substrates

Property	Unit	n-Type (Bi_2Te_3)	p-Type (Sb_2Te_3)
Panel a			
P	W/m^3 K	8.61×10^{13}	1.761×10^{13}
α_{bulk}	V/K	-228×10^{-6}	171×10^{-6}
α_b	V/K	187×10^{-6}	-252×10^{-6}
ρ_e	Ω m	1.30×10^{-5}	1.04×10^{-5}
$(A_{te}R_e)_b$	Ω m^2	2.6×10^{-12}	6.8×10^{-12}
k_p	W/m K	1.5	1.5
$(A_{te}R_c)_{b,p}$	$K/(W/m^2)$	9.2×10^{-8}	8.0×10^{-8}
k_e	W/m K	0.5	0.6
$(A_{te}R_c)_{b,e}$	$K/(W/m^2)$	3.5×10^{-7}	9.3×10^{-7}
Property	Unit	Metal connector	Substrate
Panel b			
ρ_e	Ω m	1.7×10^{-8}	–
k	W/m K	400	163

2.2. Model for the substrate and the metal connector

Thermal energy is transferred only by conduction in the substrates and metal connectors and is described by Fourier's law

$$-\nabla\cdot(k_i\nabla T)=\rho_c j_e^2, \tag{7}$$

where k_i is k_c for the metal connector, k_{cold} for the cold-side (top) substrate and k_{hot} for the hot-side (bottom) substrate. The term related to the Joule heating of the right hand side is considered only in the metal connectors and not in the substrates since the substrates should be insulated for the electricity.

The boundary conditions at the cold-side and hot-side surfaces will be the constant temperature or heat flux conditions. The interface condition between the cold-side connector and the thermoelectric element is

$$-k_{cold}\frac{\partial T}{\partial z}\bigg|_{-\frac{L_{te}}{2}}=\frac{T_c-T_p}{(A_{te}R_c)_{b,p}}\bigg|_{-\frac{L_{te}}{2}}+\frac{T_c-T_e}{(A_{te}R_c)_{b,e}}\bigg|_{-\frac{L_{te}}{2}} \tag{8}$$

and the condition between the hot-side connector and the thermoelectric element is

$$-k_{hot}\frac{\partial T}{\partial z}\bigg|_{\frac{L_{te}}{2}}=\frac{T_p-T_h}{(A_{te}R_c)_{b,p}}\bigg|_{\frac{L_{te}}{2}}+\frac{T_e-T_h}{(A_{te}R_c)_{b,e}}\bigg|_{\frac{L_{te}}{2}}. \tag{9}$$

In order to solve Eq. (7), adiabatic boundary conditions are applied to the surfaces except for the top and bottom surfaces.

2.3. Model for the thermal equilibrium

The non-equilibrium is characterized by the cooling length which is defined in terms of the electron/hole energy relaxation time, electron/hole concentration, Boltzmann constant, and electron/phonon thermal conductivities of a thermoelectric element [8]. The estimated cooling length is typically less than 1 μm so that the bulk thermoelectric element can be treated as if it is in the thermal equilibrium since the thickness of the element is much thicker than the cooling length.

The bulk type thermoelectric cooler is generally studied with thermal equilibrium condition [12] and the equilibrium model is introduced here for the comparison with the non-equilibrium model described in the previous section. In the equilibrium model, the thermal conduction within thermoelectric elements is analyzed with one equation for the equilibrium temperature. If the thermoelectric element is in thermal equilibrium ($T_p = T_e$), the equations can be derived by adding Eqs. (1) and (2) in terms of the equilibrium temperature,[2] T, defined by $kT = k_pT_p + k_eT_e$, in which $k = k_p + k_e$ [10]. Thus, the energy equation can be written as

$$-\nabla\cdot(k\nabla T)=\rho_e j_e^2. \tag{10}$$

The interface conditions for thermoelectric elements are similarly written as follows:

$$\frac{T_c-T}{(A_{te}R_c)_b}\bigg|_{-\frac{L_{te}}{2}}=-k\frac{\partial T}{\partial z}\bigg|_{-\frac{L_{te}}{2}}+\Delta\alpha j_e T|_{-\frac{L_{te}}{2}}-(A_{te}R_e)_b\frac{j_e^2}{2}, \tag{11}$$

$$\frac{T-T_h}{(A_{te}R_c)_b}\bigg|_{\frac{L_{te}}{2}}=-k\frac{\partial T}{\partial z}\bigg|_{\frac{L_{te}}{2}}+\Delta\alpha j_e T|_{\frac{L_{te}}{2}}+(A_{te}R_e)_b\frac{j_e^2}{2} \tag{12}$$

and for the metal connectors,

$$-k_{cold}\frac{\partial T}{\partial z}\bigg|_{-\frac{L_{te}}{2}}=\frac{T_c-T}{(A_{te}R_c)_b}\bigg|_{-\frac{L_{te}}{2}}, \tag{13}$$

$$-k_{hot}\frac{\partial T}{\partial z}\bigg|_{\frac{L_{te}}{2}}=\frac{T-T_h}{(A_{te}R_c)_b}\bigg|_{\frac{L_{te}}{2}}. \tag{14}$$

3. Solution method

The equations described in the previous section are solved using the COMSOL Multiphysics which is the commercial software package based on the finite element method and is applicable to multiphysics problems.

The thermophysical properties related to the thermoelectric element are evaluated by referring to the values reported in the literature [8] and are given in Table 1. The material of the metal connector is assumed to be copper for the sake of convenience. The thermal conductivities of copper and silicon are adopted from the material library of the COMSOL software.

In the calculation considering the thermal non-equilibrium near the interfaces of the thermoelectric elements, the domain for calculation is divided into two subdomains as shown in Fig. 1. The first subdomain is used for thermoelectric elements with Eqs. (1) and (2) and the second subdomain is used for metal connectors and substrates with Eq. (7). The first subdomain has two different dependent variables such as T_p, T_e and the second subdomain has only T. In the first subdomain, the equations are separately applied to the n-type and p-type elements with their own properties indicated in Table 1. The temperatures for two subdomains are connected with interface conditions, Eqs. (3)–(6) and Eqs. (8) and (9). If the thermal equilibrium is considered, the equations described as Eqs. (10)–(12) are used in the first subdomain and Eqs. (13) and (14) are used as interface conditions of metal connectors.

4. Results and discussion

4.1. Validation of the analysis

The analysis has firstly been validated with the one-dimensional analytic solution reported in the literature [8]. The analysis for validation is carried out in the

[2] The equilibrium temperature is called as a center-of-thermal-conductivity temperature which is used to match both phonon and electron temperatures of the interface in non-equilibrium with the temperature of metal connector in equilibrium [10].

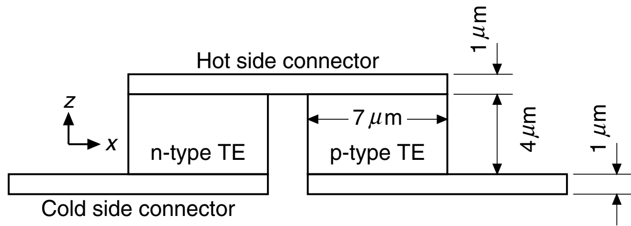

Fig. 2. Schematic of the two-dimensional geometry.

two-dimensional geometry as shown in Fig. 2. The dimension of the geometry is arbitrarily determined but the thickness of thermoelectric element is fixed to 4 μm so that the predicted results can be compared with the one-dimensional analytic solutions. The thickness of the metal connector is fixed to 1 μm and the width of the legs is fixed to 7 μm, but those dimensions are not important here since the vertical surfaces are assumed to be thermally insulated so that the temperature varies little in the x-direction. The properties of materials shown in Table 1 are used in the analysis for validation.

The solutions indicated as symbols in Fig. 3 are obtained from the one-dimensional analytic formulation [8]. The predicted temperatures are nearly identical to the one-dimensional analytic solutions as indicated in Fig. 3. The result shows that the thermal non-equilibrium near the interface causes the different temperatures for the electron and the phonon. The temperature jump for electron conduction is larger than that for phonon conduction due to the relatively large boundary resistance for electron conduction, $(A_{te}R_c)_{b,e}$, as indicated in Table 1. When the electric current does not flow, the Peltier effect does not take place and then the temperatures for the electron and phonon are identical to each other.

The analysis to compare the results for the electron–phonon thermal equilibrium and non-equilibrium near the interface is also carried out in the two-dimensional geometry as shown in Fig. 2. Fig. 4 compares the results for the thermal equilibrium and non-equilibrium analyses. For the comparison, the equilibrium temperature, $T\,(kT = k_pT_p + k_eT_e)$, is used for the non-equilibrium solution. The properties for the equilibrium model such as the boundary resistances and thermal conductivities of thermoelectric elements are averaged with values given in Table 1. The boundary resistance is written by considering the thermal conduction through the interface,

$$(A_{te}R_c)_b = \frac{(A_{te}R_c)_{b,e}(A_{te}R_c)_{b,p}}{(A_{te}R_c)_{b,e} + (A_{te}R_c)_{b,p}} \tag{15}$$

and the thermal conductivity is written as $k = k_e + k_p$ for $T_e = T_p = T$.

The temperatures for the n-type thermoelectric element are nearly identical for different currents but the temperatures for the p-type thermoelectric element show different variations for the two models as shown in Fig. 4. The average thermal conductivities are 2.0 and 2.1 W/m K, and the averaged boundary resistances are 7.29×10^{-8}

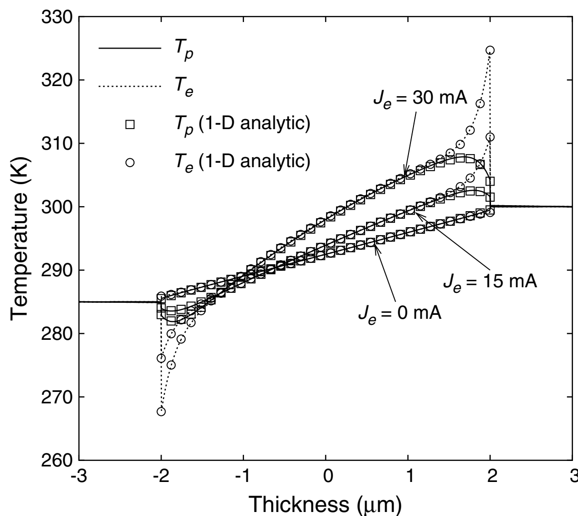

Fig. 3. Comparison of predicted temperature distributions with one-dimensional analytic solutions regenerated from the literature [8].

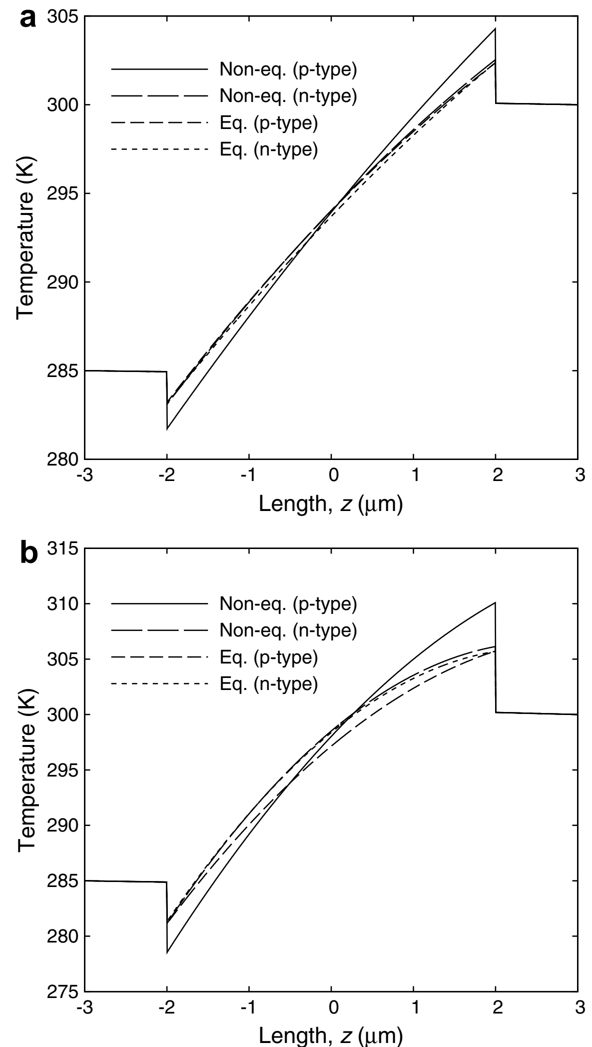

Fig. 4. Temperature distribution for the two-dimensional geometry: (a) $J_e = 15$ mA and (b) $J_e = 30$ mA.

and 7.37×10^{-8} m^2 K/W, respectively for the n- and p-type elements. Those properties do not differ much from each other and then the temperatures for n- and p-type elements in the equilibrium condition do not also differ much from each other. However, in the non-equilibrium condition, the temperature jump near the interface for electron conduction is much higher than for phonon conduction. This is primarily due to the difference between the boundary resistances for electron and phonon conduction. For the n-type element with relatively small electron boundary resistance, the temperature obtained from the non-equilibrium analysis is similar to the temperature from the equilibrium analysis.

The differences in temperatures obtained from two analyses are large for the p-type element with relatively large electron boundary resistance. It seems to be due to the electron–phonon interaction near the interface related to the boundary resistance because average conductivities differ a little and other properties are identical in the two different analyses. Thus, the electron–phonon thermal non-equilibrium near the interface is considered in the analysis of the present study.

4.2. Effect of the element thickness

The three-dimensional analysis is carried out with the geometry shown in Fig. 1 but the thickness of thermoelectric elements is changed to investigate the cooling performance of the proposed thermoelectric cooler with thickness. The thicknesses considered in the present study are 5, 10, 15, 20 μm.

In order to figure out the performance of the micro-cooler, the calculation has been carried out when the hot-side temperature is varied from 45 °C to 125 °C with the cold-side temperature fixed to 25 °C. Thus the difference between the hot-side and cold-side temperatures is varied from 20 °C to 100 °C and the predicted results are shown in Figs. 5 and 6.

The cooling rate of the cooler increases with the electric current but the rate decreases after it meets its maximum value at a certain current and the cooling rate also decreases as the temperature difference increases as shown in Fig. 5a. It is not efficient if the cooler is used at the current greater than 1.12 A since the cooling rate decreases even though the current increases. When $L_{te} = 20$ μm, the maximum cooling rate occurs at $J_e = 1.12$ A regardless of the hot-side temperature. The maximum cooling rate decreases at the constant rate by 0.113 W when the temperature difference increases by 20 °C. This trend can be found for the cases with the different thickness of the thermoelectric element shown in Fig. 7. For example, when $L_{te} = 15$ μm, the maximum cooling rate occurs at $J_e = 1.41$ A and the rate decreases by 0.148 W when the temperature difference increases by 20 °C.

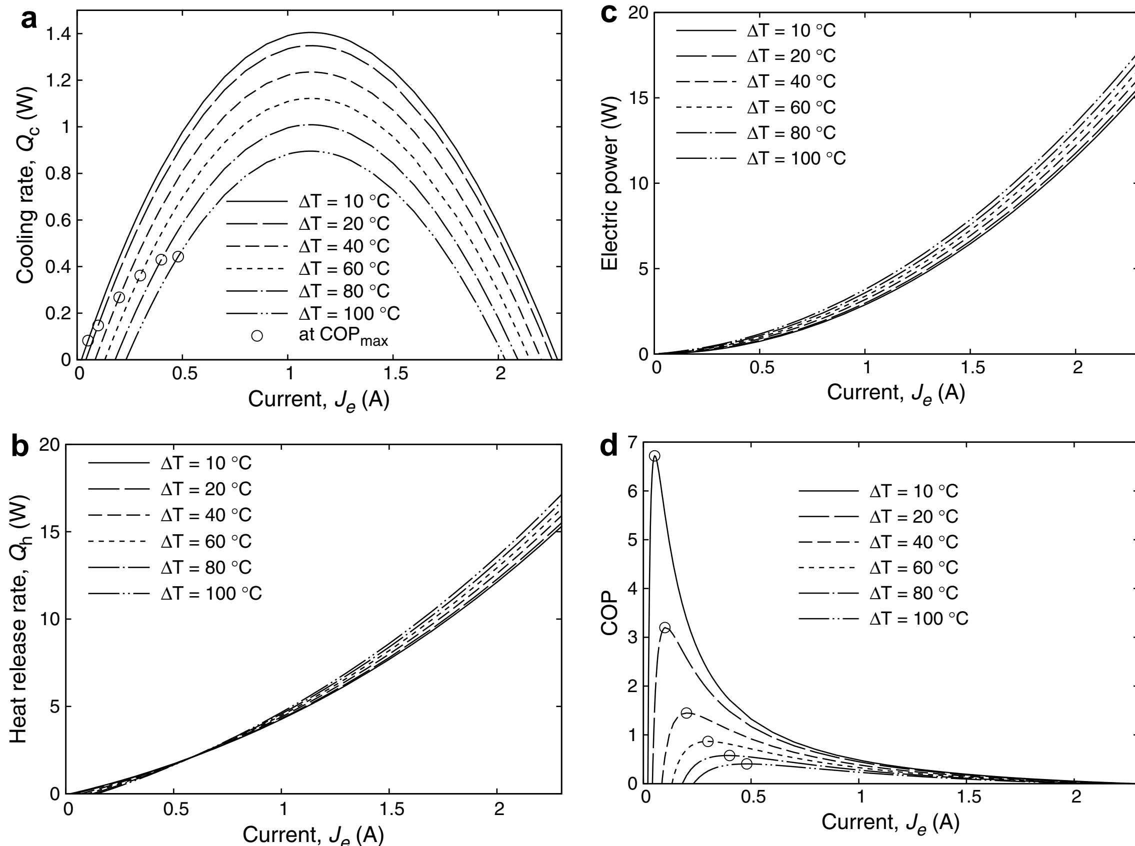

Fig. 5. Variation of (a) cooling rate at the cold side, (b) heat release rate at the hot side, (c) power, and (d) COP of the cooler ($L_{te} = 20$ μm).

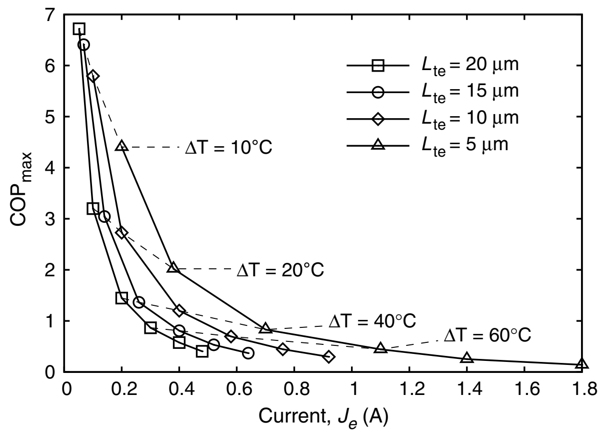

Fig. 6. Maximum coefficient of performance with the thickness of thermoelectric element.

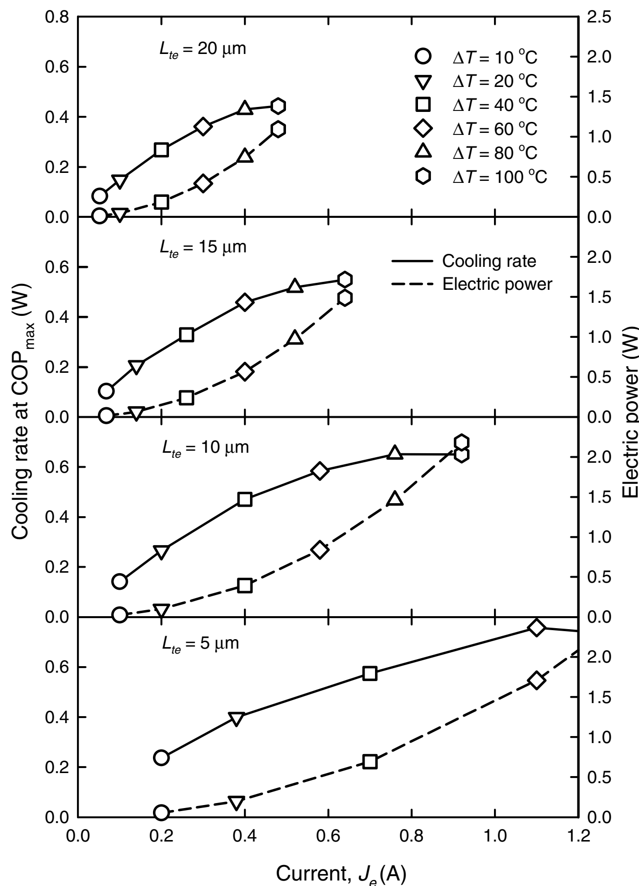

Fig. 7. Cooling rate and electric power corresponding to the maximum COP with the thickness of thermoelectric element.

The maximum cooling rate occurs when the Peltier cooling is maximized and the joule heating is minimized at the interface between the thermoelectric element and metal connector. The current density at which the maximum cooling rate occurs can be estimated from Eq. (5) and it can be written as $j_{e,max} = \Delta\alpha T_e/(A_{te}R_e)_b$. Since the Seebeck coefficients, $\Delta\alpha$, and boundary resistance, $(A_{te}R_e)_b$, are constant in the present work, the current density depends only on T_e at the interface. Moreover, since the cold-side temperature is fixed in the present work, T_e at the cold-side interface does not vary much with the hot-side temperature so that the current density is nearly constant and the current ($J_{e,max} = j_{e,max}A_{te}$) varies only with the cross-sectional area of the thermoelectric element. As the thickness of the element decreases, T_e at the cold-side interface increases and then $J_{e,max}$ increases for the fixed value of the cross-sectional area of the element.

The heat release rate gradually increases with the current even after the current ($J_e = 1.12$ A) at which the cooling rate reaches its maximum value as shown in Fig. 5b. It is not efficient that the cooler is used at the current greater than 1.12 A since the cooling rate decreases even though the current increases. The heat release rate gradually increases with the electric current applied to the cooler. In addition, the heat release rate decreases with the increase of the temperature difference for the current less than 0.77 A but the rate increases with the temperature difference for the current greater than 0.77 A.

The electric power required is evaluated by considering the thermal energy balance in the cooler as $P_e = Q_h - Q_c$. It is reasonable because all the boundaries except for the hot-side and cold-side surfaces are assumed to be thermally insulated. Since the cooling rate is fairly less than the heat release rate though the cooling rate initially increases and decreases after its maximum value with the current, the electric power required in the cooler increases with the current as like the heat release rate as shown in Fig. 5c. The power also increases as the temperature difference of the cooler increases.

Fig. 5d shows the variation of the COP of the cooler with electric current. The COP increases as the temperature difference decreases so that the smaller temperature difference gives the higher COP. The COP has its maximum value at the relatively small current in comparison to the cooling rate. When $L_{te} = 20$ μm, the maximum COP decreases from 6.72 to 0.40 and the current increases from 0.052 to 0.48 A as the temperature difference of the cooler increases from 10 to 100 °C. The maximum COP decreases quickly as the temperature difference increases. At the current at which the maximum COP occurs, the cooling rate increases from 0.082 to 0.44 W with the temperature difference as indicated with small circles in Fig. 5a. The cooling rate is less than the maximum cooling rate obtained for the current of 1.12 A. However, in order to increase the energy efficiency of the cooler, the cooler should be operated at the condition for which the maximum COP can be obtained.

Figs. 6 and 7 show variations of the maximum COP, the corresponding cooling rate and electric power for the coolers with the thermoelectric elements of different thickness. As the thickness of the element decreases, the maximum COP decreases so that the power required increases as shown in Figs. 6 and 7. The current at which the maximum

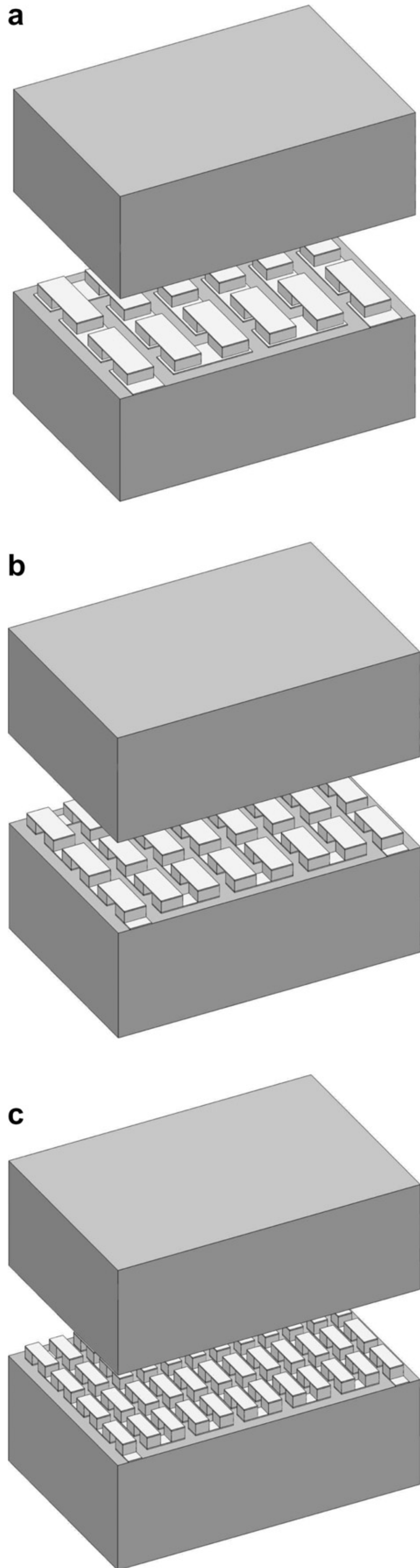

Fig. 8. Geometries of micro-coolers considered in the analysis: (a) 12 pairs, (b) 24 pairs, and (c) 48 pairs.

COP occurs also increases with the decrease of the thickness. When $\Delta T = 10\ ^\circ\mathrm{C}$, the maximum COP's are 6.72, 6.41, 5.79, and 4.4 at the current of 0.052, 0.068, 0.1, and 0.2 A for $L_{te} = 20$, 15, 10, and 5 μm, respectively. For the same thickness, the maximum COP decrease more quickly with the electric current. When the thickness is small and temperature difference is large, the current for the maximum COP largely increases. When the thickness is large, the maximum COP occurs at the relatively small current and the corresponding electric power is also small so that it may be of practical use.

The cooling rate corresponding to the maximum COP increases little by little and the operating current increases as the thickness of the element decreases for the same temperature difference. The cooling rate also increases with the increase of the temperature difference but the electric power increases much due to the decrease of the COP.

It is clear that the thickness of thermoelectric element affects the cooling performance of the micro-cooler. As the thickness of the element decreases, the maximum COP decreases and the corresponding current increases. Even though the cooling rate increases with the decrease of the thickness, the electric power required greatly increases due to the relatively low COP.

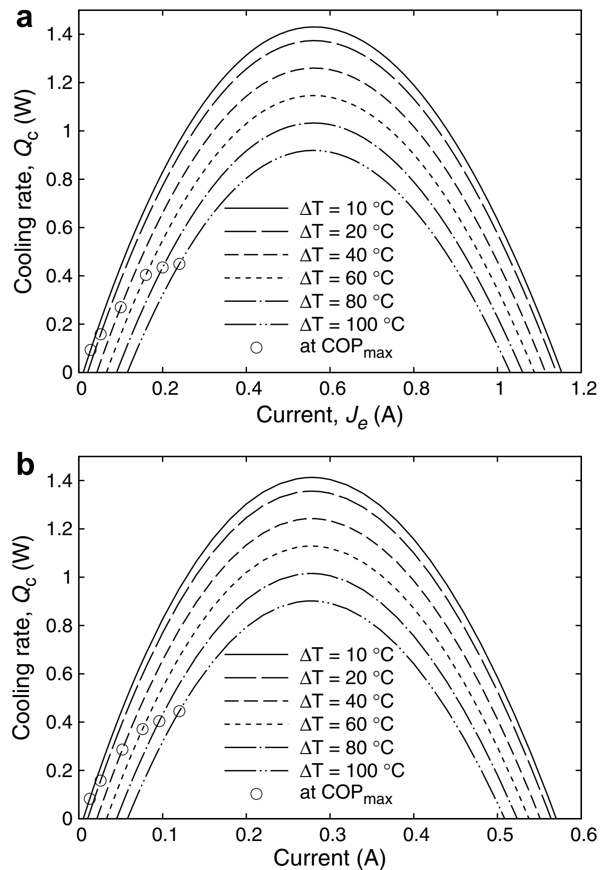

Fig. 9. Cooling rate with temperature difference between the hot- and cold-side surfaces: (a) 24 pairs and (b) 48 pairs.

4.3. Effect of the number of pairs

In order to investigate the effect of the number of pairs, the analysis has been carried out for the geometries illustrated in Fig. 8. The thickness of the elements is fixed to 20 μm and the size of each substrate is 560 μm × 380 μm × 200 μm. Any other dimensions are the same as those shown in Fig. 1. Each geometrical configuration has been constructed that the sum of cross-sectional areas of thermoelectric elements should be equal to that of other configuration. The sum of cross-sectional areas is 60,000 μm^2. Thus when the number of pairs is small, each thermoelectric element is large cross-sectional area. The cooler with 12 thermoelectric pairs has the same geometry shown in Fig. 1 so that the result for the cooler is referred to figures shown in the previous subsection. The cold-side substrates in Fig. 8 are detached from others for visual effect and those are attached in the analysis. The temperature conditions are the same as those described in the previous subsection.

The cooling rate of the cooler increases with the electric current but the rate decreases after it meets its maximum value at a certain current, and the rate decreases as the hot-side surface temperature (or temperature difference) increases as shown in Fig. 9. For the cooler with 12 thermoelectric pairs, the maximum cooling rate varies in the range from 0.9 to 1.41 W and it occurs at $J_e = 1.12$ A regardless of the temperature difference as shown in Fig. 5a. The maximum cooling rates for 24 and 48 pairs are nearly identical to those for 12 pairs since the sum of cross-sectional areas of the thermoelectric elements is the same regardless of the number of pairs and the same boundary conditions are used for all the cases. The maximum rate occurs at $J_e = 0.56$ A for 24 pairs and $J_e = 0.28$ A for 48 pairs. When the number of pairs is large, the maximum cooling rate occurs at a relatively small current since the cross-sectional area of the thermoelectric element is relatively small and then the current density becomes large for the same current.

Fig. 10 shows the variation of the COP of the cooler with the current and the temperature difference. The maximum COP increases from 0.4 to 6.7 as the temperature difference decreases. The maximum COP occurs in the range from 0.052 to 0.48 A for the case of 12 pairs in Fig. 5d, in the range from 0.028 to 0.24 A for the case of 24 pairs and in the range from 0.013 to 0.12 A for the case of 48 pairs in Fig. 10. It indicates that the maximum COP occurs at the same current density regardless of the number of pairs. The cross-sectional area of each thermoelectric element for the cooler with 12 pairs is 4 times larger than that for the cooler with 48 pairs so that the current density in the cooler with 12 pairs is one-fourth as large as that in the

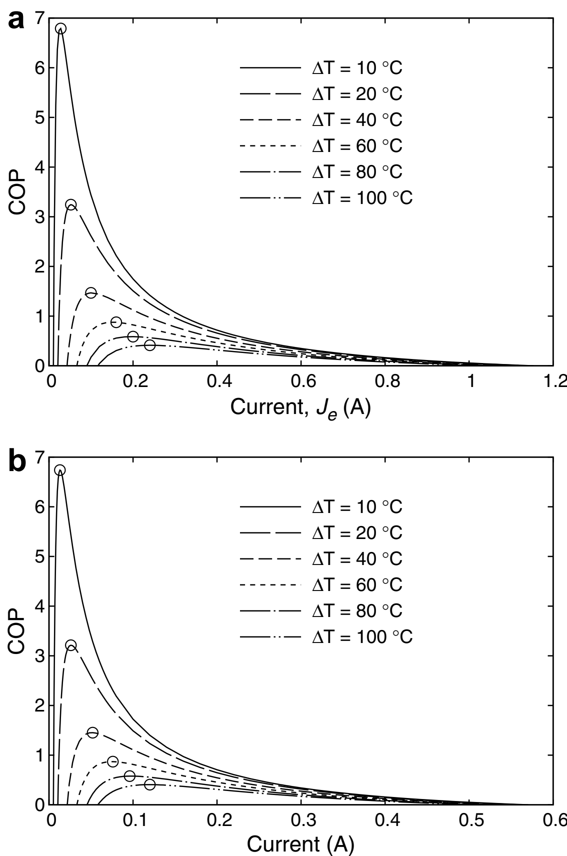

Fig. 10. Coefficient of performance with temperature difference between the hot- and cold-side surface: (a) 12 pairs and (b) 48 pairs.

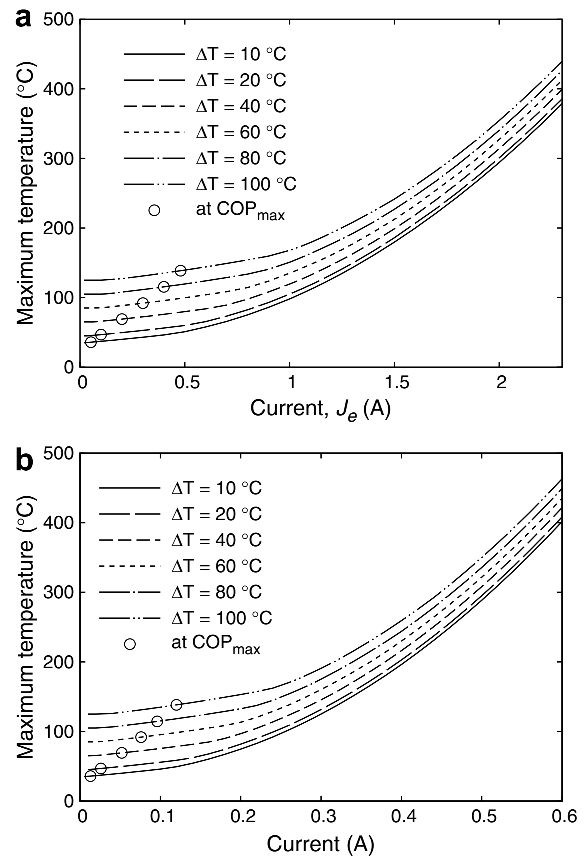

Fig. 11. Maximum temperature variations with electric current: (a) 12 pairs and (b) 48 pairs.

cooler with 48 pairs for the same current applied. Thus, the result shows that the cross-sectional area of the element is an important factor to determine the operating current and the area directly affects the Peltier cooling/heating through the current density.

The maximum temperature is observed in the interface between the element and the hot-side connector where the Peltier heating takes place as shown in Fig. 3. Fig. 11 shows that the maximum temperature slowly increases in the range of 30–150 °C with the current less than that where the maximum cooling rate occurs, but after the current the temperature promptly increases. The maximum temperature quickly increases at the smaller current when the temperature difference is small. Thus, Fig. 11 explains that the cooler can be damaged due to high temperature when the operating current of the thermoelectric micro-cooler is large.

4.4. Relationship of parameters

The results in the previous subsection are obtained for different number of pairs but the element thickness and the sum of cross-sectional areas are fixed. The results shows that the parameters obtained from the analysis are identical when those are plotted with current density ($j_e = J_e/A_{te} = J_e N_{te}/\sum A_{te}$) regardless of the number of pairs. The relationships shown in Fig. 12 can be drawn when the thickness of thermoelectric elements is 20 μm and the sum of the cross-sectional areas of thermoelectric pairs are fixed to 6000 μm^2. The operating current can be obtained from the current density and the cross-sectional area of a element. For a given current density, a small cross-sectional area of a element (A_{te}) results in the large number of thermoelectric pairs (N_{te}) since the sum of cross-sectional areas ($\sum A_{te}$) is fixed in the present results.

Fig. 12a shows that the relationship of the COP and cooling rate with the current density and temperature difference of the cooler. If the current density and temperature difference are selected, the COP and cooling rate are determined with this figure. Fig. 12b shows that the relationship of the voltage and cooling rate with temperature difference and current density. This figure gives the voltage and cooling rate for given temperature difference and current density. The voltage has the similarity when it is divided by the cross-sectional area of a element as the current does. If the voltage is determined, the power required in the cooler is easily estimated and the heat release rate can sequentially be estimated.

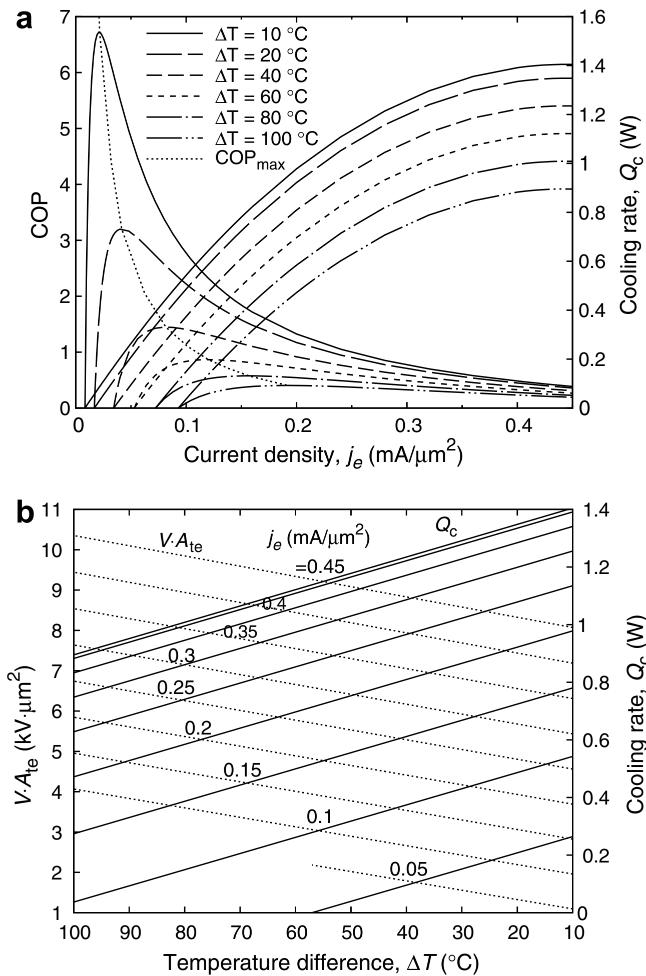

Fig. 12. Relationships of (a) COP and cooling rate with current density and operating current density, and (b) voltage and cooling rate with temperature difference and current density ($L_{te} = 20$ μm, $\sum A_{te} = 60{,}000$ μm^2).

5. Conclusion

The three-dimensional numerical analysis has been carried out using the COMSOL Multiphysics software package to figure out the cooling performance of the thermoelectric micro-cooler. The small-size and column-type thermoelectric cooler is considered and Bi_2Te_3 and Sb_2Te_3 are selected as the n- and p-type thermoelectric materials, respectively. The thickness of the thermoelectric element considered is 5–20 μm.

The validation has been carried out with the two-dimensional geometry and the predicted temperature is in good agreement with the one-dimensional analytic solution given in the literature. The electron–phonon thermal equilibrium and non-equilibrium is considered in the two-dimensional analysis near the interface between the connector and the thermoelectric element. In this case, the temperatures obtained from two types of analyses differ especially in the p-type element.

The effect of parameters such as the temperature difference, the current, and the thickness of the thermoelectric element on the performance of the cooler has been investigated. The COP has the maximum value at a certain current and the value increases with the decrease of temperature difference or the increase of the thickness. The predicted results show that the performance can be improved more for thick thermoelectric elements at the small temperature difference and small current.

The maximum cooling rate occurs at a certain current and the rate is large when the temperature difference is

relatively small. The current at which the cooling rate is maximized is relatively small when the thickness of thermoelectric element is large. The COP has the maximum at the current less than that where the cooling rate is maximized. The maximum COP is also large when the temperature difference is small but the current corresponding to the maximum COP is large when the temperature difference is large.

It is clear that the thickness of thermoelectric element affects the cooling performance of the micro-cooler. As the thickness of the element decreases, the maximum COP decreases and the corresponding current increases. Even though the cooling rate increases with the decrease of the thickness, the electric power required greatly increases due to the relatively low COP.

The maximum COP occurs at the same current density regardless of the number of pairs and thus the current corresponding to the maximum COP decreases as the number of pairs increases since the cross-sectional area of the thermoelectric element decreases with the number of pairs. The cross-sectional area of the element is an important factor to determine the operating current since the area directly affects the Peltier cooling/heating through the current density.

The cooling rate is fairly less than the heat release rate, the electric power increases with the current. The device would be operated at the small current where the COP is maximized. The maximum temperature which is observed in the interface between the thermoelectric element and the hot-side connector slowly increases at the small current but the temperature promptly increases as the current increases.

Finally, the relationships of the parameters related to the performance and design of the micro-cooler are drawn and it can be utilized to figure out its performance or to design the micro-cooler.

Acknowledgements

This research is implemented as a part of the project "Development of Technology for Advanced Cooling System" managed by Korea Research Council for Industrial Science and Technology. The authors gratefully appreciate the support.

References

[1] D.M. Rowe (Ed.), Handbook of Thermoelectrics, CRC Press, Boca Raton, 1995.

[2] H. Böttner, Thermoelectric micro devices: current state, recent developments and future aspects for technological progress and applications, in: Proceedings of 21st International Conference on Thermoelectrics, Long Beach, CA, USA, 2002, pp. 511–518.

[3] J.R. Lim, G.J. Snyder, C.-K. Huang, J.A. Herman, M.A. Ryan, J.-P. Fleurial, Thermoelectric microdevice fabrication process and evaluation at the Jet Propulsion Laboratory (JPL), in: Proceedings of 21st International Conference on Thermoelectrics, Long Beach, CA, USA, 2002, pp. 535–539.

[4] D.-J. Yao, C.-J. Kim, J.L. Liu, K.L. Wang, J. Snyder, J.-P. Fleurial, G. Chen, MEMS thermoelectric microcooler, in: Proceedings of 20th International Conference on Thermoelectrics, Beijing, PR China, 2001, pp. 401–404.

[5] D.J. Yao, G. Chen, C.-J. Kim, Low temperature eutectic bonding for in-plane type micro thermoelectric cooler, in: Proceedings of International Mechanical Engineering Congress and Exposition, New York, USA, 2001, Paper No. IMECE2001/MEMS-23901.

[6] G.J. Snyder, J.R. Lim, C.-K. Huang, J.-P. Fleurial, Thermoelectric microdevice fabricated by a MEMS-like electrochemical process, Nature Mater. 2 (8) (2003) 528–531.

[7] H. Böttner, J. Nurnus, A. Gavrikov, G. Kühner, M. Jägle, C. Künzel, D. Eberhard, G. Plescher, A. Schubert, K.-H. Schereth, New thermoelectric components using microsystem technologies, J. Microelectromech. Syst. 13 (3) (2004) 414–420.

[8] L.W. da Silva, M. Kaviany, Micro-thermoelectric cooler: interfacial effects on thermal and electrical transport, Int. J. Heat Mass Transfer 47 (10–11) (2004) 2417–2435.

[9] L.W. da Silva, M. Kaviany, M. Asheghi, Measured performance of a micro thermoelectric cooler, in: Proceedings of ASME HT-FED 2004, Charlotte, NC, USA, 2004, Paper No. HT-FED2004-56412.

[10] M. Bartkowiak, G.D. Mahan, Heat and electricity transport through interfaces, Recent Trends in Thermoelectric Materials, Vol. II, Semiconductors and Semimetals, vol. 70, Academic Press, New York, 2001, pp. 245–271.

[11] Y.G. Gurevich, O.L. Mashkevich, The electron–phonon drag and transport phenomena in semiconductors, Phys. Rep. (Rev. Sect. Phys. Lett.) 181 (6) (1989) 327–394.

[12] D.-J. Yao, C.-J. Kim, G. Chen, J.-P. Fleurial, H.B. Lyon, Spot cooling by using thermoelectric microcooler, in: Proceedings of 18th International Conference on Thermoelectrics, Baltimore, MD, USA, 1999, pp. 256–259.